

## Interaction parameters and a quenched-disorder phase diagram for $(\text{GaAs})_{1-x}\text{Ge}_{2x}$ alloys

Roberto Osório\* and Sverre Froyen

*National Renewable Energy Laboratory, Golden, Colorado 80401*

(Received 21 July 1992)

We obtain the interaction parameters for the spin-1 Ising representation of  $(\text{GaAs})_{1-x}\text{Ge}_{2x}$  metastable alloys, based on the total energies of a set of ordered structures calculated by the first-principles self-consistent pseudopotential method. We then use these parameters to reexamine the thermodynamic consequences of a recently proposed quenched-disorder model for the observed zinc-blende-to-diamond phase transition in  $(\text{GaAs})_{1-x}\text{Ge}_{2x}$ . In this model, Ge atoms are distributed at random at all lattice sites. We present a complete phase diagram of the quenched-disorder model in the pair approximation of the cluster-variation method. In view of our set of first-principles interaction parameters, we conclude that, like previously proposed bulk thermodynamic models, the quenched-disorder model does *not* lead to a phase transition that agrees with the experimental result.

### I. INTRODUCTION

The measured *equilibrium* phase diagram of  $(\text{GaAs})_{1-x}\text{Ge}_{2x}$  (Ref. 1) shows that there is nearly total phase separation into  $(1-x)$  GaAs and  $x$  Ge at all temperatures below melting. On the other hand, single-phase  $(\text{GaAs})_{1-x}\text{Ge}_{2x}$  [and other  $(A^{\text{III}}B^{\text{V}})_{1-x}C_{2x}^{\text{IV}}$ ] alloys have been synthesized by *nonequilibrium* growth methods,<sup>2</sup> producing compounds with either the zinc-blende symmetry of the GaAs constituent or the diamond symmetry of the Ge constituent. A continuous phase transition from the zinc-blende to the diamond symmetry has been observed at a composition  $x_c \approx 0.3-0.4$  (Refs. 3-5).

The *equilibrium* segregating (two-phase) behavior of GaAs and Ge is caused by the high energy ( $E_b \gtrsim 100$  meV) that would have been necessary to form nonoctet Ga-Ge and As-Ge "bad" bonds in single-phase alloys.<sup>6</sup> Each of these bonds has a total number of valence electrons that deviates by  $\Delta Z_v = \pm 1$  from the normal octet Ga-As and Ge-Ge bonds present in the constituents. The average energy of a third type of bonds, the so-called "wrong" bonds, Ga-Ga and As-As, whose average number of electrons deviates by  $\Delta Z_v = \pm 2$  from the octet bonds, is usually estimated to be  $E_w = (3-4)E_b$ .<sup>7-9</sup>

A series of works<sup>3,10,11</sup> attempted to understand the order-disorder (zinc-blende to diamond) transition in nonequilibrium  $(\text{GaAs})_{1-x}\text{Ge}_{2x}$  alloys in terms of stable or metastable features of the bulk phase diagram. The results of such thermodynamic theories can be summarized as follows: (i) If wrong ( $\Delta Z_v = \pm 2$ ) bonds are permitted in the model, the interaction parameters can be adjusted to lead to a critical concentration  $x_c \approx 0.3$  (Refs. 3, 10, and 11). (ii) If no wrong bonds are allowed in the model, the critical concentration is always  $x_c > 0.57$ , in a phase diagram obtained in the pair approximation of the cluster-variation method (CVM).<sup>11</sup> (iii) In both approaches one finds practically complete phase separation

at  $T \lesssim 1500$  K if, instead of fitting the interaction parameters, one calculates them from a realistic first-principles model.<sup>6</sup> This result is a consequence of  $E_b \gtrsim 100$  meV and is found whether one assumes  $E_w \rightarrow \infty$  (i.e., no wrong bonds) or  $E_w \approx 3-4 E_b$  (which, at  $T \lesssim 1500$  K, leads to a very small number of wrong bonds). However, all previous theoretical studies have assumed equal interactions for the Ga-Ge and As-Ge bonds, as well as for the higher-energy Ga-Ga and As-As bonds, when present. The previous results were therefore based on the hypothesis of invariance with respect to the interchange  $\text{Ga} \leftrightarrow \text{As}$ .

Recently, Gu, Ni, and Zhu<sup>12</sup> studied the thermodynamic consequences of removing this  $\text{Ga} \leftrightarrow \text{As}$  symmetry in a model that used pairwise interactions obtained from the universal-parameter tight-binding (UPTB) method.<sup>13</sup> These pairwise energies strongly favor As-As over Ga-Ga bonds. The resulting equilibrium phase diagram, also obtained in the CVM pair approximation, still shows that nearly total phase separation is the thermodynamically stable configuration at all temperatures below melting. Gu, Ni, and Zhu then proposed that the order-disorder transition could be explained in terms of a model that we call the "quenched-disorder model." The idea is to simulate the nonequilibrium nature of the alloy by assuming that the Ge atoms are distributed with equal probability (given by the composition  $x$ ) on all lattice sites, regardless of the occupation of the neighboring sites. This assumption precludes the otherwise thermodynamically favored phase separation into a GaAs-rich and a Ge-rich phase. The quenched-disorder model gives a phase diagram with a single second-order phase-transition curve between the zinc-blende and the diamond phases. At typical preparation temperatures, the critical concentration for the UPTB parameters is  $x_c \approx 0.36-0.37$ , in agreement with the experimental values  $0.3-0.4$  (Refs. 4 and 5).

Since UPTB does not always give reliable quantitative

information, we decided to obtain independently pairwise interaction parameters for  $(\text{GaAs})_{1-x}\text{Ge}_{2x}$ , based on first-principles pseudopotential calculations. We find interaction parameters that favor Ga-Ga bonds over As-As bonds, in opposition to the result obtained with UPTB parameters. This result does not significantly affect the *equilibrium* phase diagram at solid-state temperatures, still leading to nearly total phase separation. We also calculate a complete phase diagram for the quenched-disorder model, which shows that the UPTB parameters correspond to a very special point of the phase diagram. Our first-principles parameters lead, at a preparation temperature  $\sim 700$  K (Ref. 4), to  $x_c \approx 0.67$  in the CVM pair approximation. We estimate that improving the statistical treatment could reduce  $x_c$  to 0.57, still larger than the experimental values 0.3–0.4. We conclude that neither the introduction of Ga $\leftrightarrow$ As asymmetry nor the quenched-disorder model explains the existence of a low-temperature single-phase alloy with a zinc-blende-to-diamond transition at  $x_c \approx 0.3$ –0.4.

In the following sections, we describe the spin-1 Ising model commonly used for the thermodynamics of ternary alloys and its ground-state diagram when applied to a general  $(AB)_{1-x}C_{2x}$  alloy (Sec. II). To investigate the Ga $\leftrightarrow$ As asymmetry, we calculate the total energy of six new ordered structures that contain wrong bonds. These are used together with previously obtained structures to provide a set of realistic interaction parameters (Sec. III). We then discuss the assumptions inherent in the quenched-disorder model, obtain its ground states (Sec. IV), and present its complete phase diagram (Sec. V). We finally analyze the implications of this model in view of our set of interaction parameters (Sec. VI).

## II. APPLYING THE BLUME-EMERY-GRIFFITHS MODEL TO $(\text{GaAs})_{1-x}\text{Ge}_{2x}$

Let us first consider a general  $(AB)_{1-x}C_{2x}$  alloy in the diamond lattice. If  $AB$  and  $C$  are lattice-matched constituents [as in  $(\text{GaAs})_{1-x}\text{Ge}_{2x}$ ], relaxation effects are expected to be less important than “chemical” interatomic energies and we assume that the alloy is described by a Hamiltonian that includes only nearest-neighbor atomic interactions (for  $A$ - $A$ ,  $B$ - $B$ ,  $C$ - $C$ ,  $A$ - $B$ ,  $A$ - $C$ , and  $B$ - $C$  pairs). This model can be exactly mapped<sup>14</sup> into the generalized spin-1 Ising, or Blume-Emery-Griffiths, Hamiltonian

$$\mathcal{H}_{\text{BEG}} = J \sum_{\langle ij \rangle} S_i S_j + K \sum_{\langle ij \rangle} S_i^2 S_j^2 + L \sum_{\langle ij \rangle} (S_i^2 S_j + S_i S_j^2), \quad (1)$$

where the spin-1 Ising variables can take the values

$$S_i = \begin{cases} 1 & \text{for } A \\ -1 & \text{for } B \\ 0 & \text{for } C \end{cases} \quad (2)$$

and the indices  $\langle ij \rangle$  indicate sums over nearest-neighbor pairs of sites. We assume a given concentration of each of the three species, so that chemical-potential terms can be

safely omitted from Eq. (1). The terms containing  $J$  and  $K$ , together with a magnetic-field (which maps into the chemical potential of species  $C$ ) term, constitute the original Blume-Emery-Griffiths (BEG) Hamiltonian,<sup>15</sup> used to model tricritical behavior in  $\text{He}^3$ - $\text{He}^4$  mixtures.

The BEG parameters are expressed in terms of interatomic nearest-neighbor pair energies  $\varepsilon_{SS'}$  ( $S, S' = A, B$ , or  $C$ ) as<sup>14</sup>

$$J = \frac{1}{4}(\varepsilon_{AA} + \varepsilon_{BB} - 2\varepsilon_{AB}), \quad (3a)$$

$$K = J - \varepsilon_{AC} - \varepsilon_{BC} + \varepsilon_{AB} + \varepsilon_{CC}, \quad (3b)$$

$$L = \frac{1}{4}(\varepsilon_{AA} - \varepsilon_{BB} - 2\varepsilon_{AC} + 2\varepsilon_{BC}). \quad (3c)$$

The pair energy  $\varepsilon_{SS'}$  represents the total energy per nearest-neighbor pair of a zinc-blende structure with only atoms  $S$  in one sublattice and only atoms  $S'$  in the other. The average wrong-bond ( $\Delta Z_v = \pm 2$ ) energy (with respect to the normal  $A$ - $B$  bond) is  $E_w = 2J$  [see Eq. (3a)]. The average bad-bond ( $\Delta Z_v = \pm 1$ ) energy, with respect to the average normal bond, is  $E_b = (J - K)/2$  [see Eq. (3b)]. The parameter  $L$  in Eq. (3c) describes the Ga $\leftrightarrow$ As asymmetry.

The Hamiltonian of Eq. (2) can be minimized in a straightforward way with respect to the probabilities  $p_{SS'}$  of finding species  $S$  and  $S'$  (regardless of orientation, i.e.,  $p_{SS'} = p_{S'S}$ ) on a nearest-neighbor pair of sites, at a fixed concentration  $x$  in  $(AB)_{1-x}C_{2x}$ . The use of this procedure in combination with a common-tangent construction leads to the ground-state diagram of Fig. 1. We assume  $J > 0$ , which corresponds to a tendency towards ordering within the  $AB$  component [rather than phase separation into  $A$  and  $B$ ; see Eq. (3a)]. Each region of this phase diagram is labeled according to the sequence of stable phases as  $x$  increases from 0 to 1. Besides the constituent phases  $AB$  (at  $x=0$ ) and  $C$  (at  $x=1$ ), the following phases are found: (i)  $ABC_2$  (at  $x = \frac{1}{2}$ ), which corresponds to the “staggered quadrupolar phase”<sup>16,17</sup> of the spin-1 model and has  $C$  atoms occupying one sublattice and  $A$  and  $B$  atoms randomly distributed in the

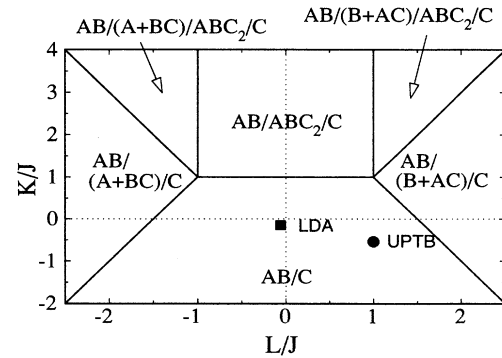


FIG. 1. Ground states of the generalized Blume-Emery-Griffiths model [Eq. (1)] for  $(AB)_{1-x}C_{2x}$  alloys. The circle (UPTB) and the small square (LDA) indicate the parameters obtained by Gu, Ni, and Zhu (Ref. 12) and in the present work, respectively.

other sublattice, and (ii)  $B + AC$  (and its complementary  $A + BC$ , both at  $x = \frac{1}{3}$ ), which corresponds to phase separation between  $A$  ( $B$ ) and the zinc-blende structure  $BC$  ( $AC$ ).

All estimates<sup>6-9,12</sup> for the interatomic pair energies in  $(\text{GaAs})_{1-x}\text{Ge}_{2x}$  lead to values  $J - K > 0$  (i.e.,  $K/J < 1$  in the ground-state diagram). When  $|L| < (3J - K)/2$ , values  $E_b > 0$  correspond in the ground-state diagram to the region  $AB/C$ , where GaAs and Ge are phase separated. We indicate in the ground-state diagram of Fig. 1 the location of the BEG energy parameters obtained by Gu, Ni and Zhu (UPTB), together with the parameters obtained in the present work (LDA).

### III. OBTAINING THE INTERACTION PARAMETERS FOR $(\text{GaAs})_{1-x}\text{Ge}_{2x}$

We have previously<sup>6</sup> modeled the energy of a system containing normal and nonoctet “bad” ( $\Delta Z_v = \pm 1$ ) bonds [but no “wrong” ( $\Delta Z_v = \pm 2$ ) bonds] by considering  $(\text{GaAs})_p/(\text{Ge}_2)_p$  superlattices (SL’s) for several orientations and repeat periods. The excess energies of such SL’s (with respect to phase separation into pure GaAs and pure Ge) were calculated<sup>20</sup> using the first-principles self-consistent-pseudopotential method. The excess energies were then fitted by a Hamiltonian that consists of a sum of Ising-like nearest-neighbor interactions between atoms and a Madelung energy term. Both contributions include effects of *charge transfer* between donor-like As-Ge bonds and acceptorlike Ga-Ge bonds. These effects lower considerably the formation energies of superlattices. The Madelung term represents the screened electrostatic interactions between compensation charges located near the Ga-Ge bonds and the As-Ge bonds. We modeled this term by placing the compensation charges ( $\pm e/4$  for full charge transfer) at the midpoints of the nonoctet bonds.

Although the Madelung contribution can be significant to the excess energies of some SL’s, we found that, for the *alloy*, by far the predominant effect of charge transfer in a composition-temperature phase diagram is produced by appropriately scaling down the Ising terms. This justifies using the BEG Hamiltonian of Eq. (1) to represent the excess energy of the alloy. We obtained the value 109 meV for the effective average bad-bond ( $\Delta Z_v = \pm 1$ ) energy  $E_b$  in  $(\text{GaAs})_{1-x}\text{Ge}_{2x}$  with charge transfer. We now supplement this analysis by considering new ordered structures that are not invariant under the interchange  $\text{Ga} \leftrightarrow \text{As}$ . In stoichiometric  $(\text{GaAs})_{1-x}\text{Ge}_{2x}$  this can only occur in structures that contain wrong ( $\Delta Z_v = \pm 2$ ) bonds. For instance, a larger number of Ga-Ge than As-Ge bonds has to be counterbalanced by more As-As than Ga-Ga bonds so that the total concentration of Ga and As remains the same. The new structures can therefore provide information not only about the  $\text{Ga} \leftrightarrow \text{As}$  asymmetry parameter  $L$ , but also about the wrong-bond energy  $E_w = 2J$ .

Three of the new structures are shown in Fig. 2; the other three are obtained by swapping  $\text{Ga} \leftrightarrow \text{As}$ . Structures (a), (b), and (c) contain, respectively, one, two, and three wrong As-As bonds per 16 atoms and have

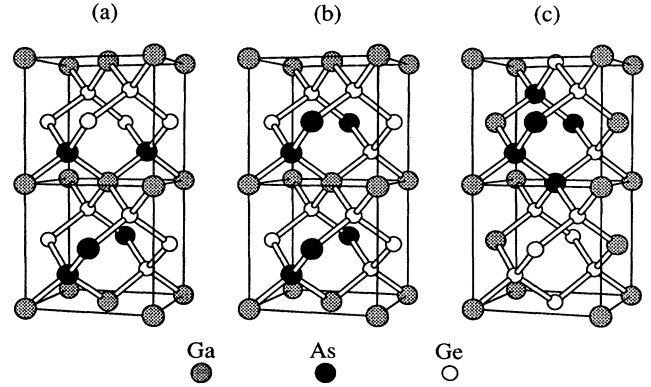


FIG. 2. New structures used to obtain the  $\text{Ga} \leftrightarrow \text{As}$  asymmetry parameter  $L$  and the “wrong-bond” energy  $E_w$ .

been constructed from the  $1 \times 1$  [001] SL by swapping the atoms of one or two Ga-Ge or As-Ge pairs of the 16-atom unit cell. We obtained the total energies of the new structures  $s$  with respect to the originating  $1 \times 1$  [001] SL, which we call  $s_0$ , using ten special  $\mathbf{k}$  points in the irreducible part of the fcc Brillouin zone. For consistency with the previous fit for  $E_b$ , relaxation effects were not included. [Relaxation decreases the formation energy of the lattice-matched  $(\text{GaAs})_p/(\text{Ge}_2)_p$  SL’s usually by less than 10%.]

We express the excess energy of these structures  $s$  with respect to phase separation as

$$\Delta E(s) = \Delta H_{\text{BEG}}(s) + \alpha E_{\text{Mad}}(s), \quad (4)$$

where the Madelung energy  $E_{\text{Mad}}(s)$  of each structure is calculated by assigning full compensation charges  $e/2$  to As-As,  $-e/2$  to Ga-Ga,  $e/4$  to As-Ge, and  $-e/4$  to Ga-Ge bonds. We found that the presence of wrong bonds makes these structures metallic. The Madelung energy is therefore scaled down (by a fitting factor  $\alpha$ ) with respect to that calculated by the above scheme, because of more effective screening and less than complete charge transfer due to metallization. The approximations involved in the Madelung energy model and its homogeneous scaling down only affect the fit of  $E_w = 2J$ , since we use the known value of  $E_b = (J - K)/2$  from our previous fit,<sup>6</sup> which did not involve structures with “wrong” bonds, and since the value of  $L$  is obtained from the energy differences between each of the structures (a)–(c) and its complementary.

To fit  $J$  and  $L$  we use Eq. (4) and the corresponding equation for the  $1 \times 1$  [001] SL, which we denote by  $s_0$  (which has  $\alpha = 1$ , since it has no wrong bonds and full charge transfer is present). We thus have

$$\begin{aligned} \Delta H_{\text{BEG}}(s) - \Delta H_{\text{BEG}}(s_0) &= \Delta E(s) - \Delta E(s_0) \\ &\quad - \alpha E_{\text{Mad}}(s) + E_{\text{Mad}}(s_0), \end{aligned} \quad (5)$$

where  $E_{\text{Mad}}(s_0)$  was calculated to be  $-4.4$  meV. The expressions for  $\Delta H_{\text{BEG}}(s) - \Delta H_{\text{BEG}}(s_0)$  in terms of the BEG parameters, the directly calculated values of

TABLE I. Expressions for  $\Delta H_{\text{BEG}}(s) - \Delta H_{\text{BEG}}(s_0)$  in terms of the parameters of Eq. (1), the directly calculated values of the total-energy differences  $\Delta E(s) - \Delta E(s_0)$ , and the model Madelung energies  $E_{\text{Mad}}(s)$  (assuming full charge transfer) for the structures  $s = (a)-(c)$  in Fig. 2 and their complementary  $(a')-(c')$ , where  $s_0$  refers to the  $1 \times 1$  [001] superlattice.

Structure $s$	$\Delta H_{\text{BEG}}(s) - \Delta H_{\text{BEG}}(s_0)$ (per atom)	$\Delta E(s) - \Delta E(s_0)$ (meV/atom)	$E_{\text{Mad}}(s)$ (meV/atom)
(a)	$(3J - K - 2L)/16$	39.1	-3.9
(a')	$(3J - K + 2L)/16$	36.1	-3.9
(b)	$(3J - K - 2L)/8$	79.9	-7.7
(b')	$(3J - K + 2L)/8$	73.3	-7.7
(c)	$(7J - K - 6L)/16$	103.7	24.9
(c')	$(7J - K + 6L)/16$	96.3	24.9

$\Delta E(s) - \Delta E(s_0)$ , and the values for  $E_{\text{Mad}}(s)$  (with  $\alpha = 1$ ) for the the six structures  $s$  are given in Table I.

The best fit of the BEG parameters, with  $(J - K)/2$  fixed at 109 meV (Ref. 6), gives  $J = 189$  meV,  $L = -11$  meV, and  $\alpha = 0.44$ . The three energy differences between each structure  $s$  and its complementary  $s'$  give values of  $L$  consistently between  $-13$  and  $-10$  meV.

A recent *ab initio* molecular-dynamics simulation of liquid GaAs found a preference for Ga-Ga over As-As bonds.<sup>21</sup> Our negative value of  $L$  implies that Ga-Ga pairs are indeed favored with respect to As-As pairs in crystalline  $(\text{GaAs})_{1-x}\text{Ge}_{2x}$ . This conclusion disagrees with the UPTB results, which show a strong preference for As-As pairs. We find a small ratio  $L/J = -0.06$ . In Table II we compare the UPTB results (line 1) to those obtained by recent first-principles self-consistent pseudopotential calculations for pure GaAs ( $E_w$  in lines two and three) and for  $(\text{GaAs})_{1-x}\text{Ge}_{2x}$  ordered structures (lines four and five). (The somewhat larger value for the result of Ref. 19 on line three may be due to the presence of negative-energy third-neighbor wrong bonds in their fit.) It is clear that the UPTB parameters work reasonably well for  $E_w$  and  $E_b$ , but produce the wrong sign and a too large magnitude of  $L/J$ .

For the typical values  $E_b \gtrsim 100$  meV, nearly total phase separation persists at preparation temperatures

TABLE II. Recent calculations for the energies  $E_b = (J - K)/2$  [of "bad"  $\Delta Z_v = \pm 1$  bonds] and  $E_w = 2J$  [of "wrong"  $\Delta Z_v = \pm 2$  bonds] and for the interaction parameter ratio  $L/J$ , for  $(\text{GaAs})_{1-x}\text{Ge}_{2x}$  alloys.

Reference	$E_b$ (meV)	$E_w$ (meV)	$L/J$
UPTB <sup>a</sup>	115	298	1.00
LDA <sup>b</sup>		360	
LDA <sup>c</sup>		463	
LDA <sup>d</sup>	100	330	
LDA <sup>e</sup>	109	378	-0.06

<sup>a</sup> Reference 12.

<sup>b</sup> Pure GaAs, Ref. 18.

<sup>c</sup> Pure GaAs, Ref. 19.

<sup>d</sup> Reference 9.

<sup>e</sup> Present work. The result for  $E_b$  was obtained in Ref. 6.

( $\sim 700$  K in Ref. 4) for both  $L \approx 0$  (Ref. 6) and  $L = 1$  (Ref. 12). Thermodynamic equilibration of the BEG model therefore cannot describe correctly the state of single-phase  $(\text{GaAs})_{1-x}\text{Ge}_{2x}$  alloys or the observed order-disorder transition at  $x_c \approx 0.3-0.4$ . In these alloys, Ge is distributed equally in all lattice sites, even when the alloy has zinc-blende symmetry, since ordering only affects the positioning of Ga and As (not Ge) in the two sublattices. Gu, Ni, and Zhu<sup>12</sup> used this fact to propose the quenched-disorder model discussed in the next section.

#### IV. THE QUENCHED-DISORDER MODEL AND ITS GROUND STATE

In the quenched-disorder model,<sup>12</sup> the probability of occupation of each lattice site by Ge is given by the concentration  $x$ , *independently of the occupation of neighboring sites*. The model supposes that Ga and As are free to equilibrate in the set of sites complementary to the sites occupied by the quenched random distribution of Ge. This assumption is very different from the situation of thermodynamic equilibrium of the three species (even in a metastable state), which was assumed in previous models.<sup>3,10,11</sup> In fact, the tendency towards phase separation implies that, even in the one-phase regions of the equilibrium phase diagram, the probabilities for finding Ge-Ge and  $X-X'$  pairs (where  $X$  and  $X'$  denote non-Ge atoms, i.e., Ga or As) are larger than their random values  $x^2$  and  $(1-x)^2$ , respectively, while the probability for finding Ge- $X$  pairs is less than its random value  $2x(1-x)$ . The assumption of a random uncorrelated distribution of Ge therefore cannot be motivated by the true *energetics* of Ge, Ga, and As atoms. It corresponds instead to a situation where the interaction energies are all zero. However, since the model can be motivated by the experimental quick quench of Ge atoms in a highly mixed state during the growth process, and since, if UPTB interactions are used,<sup>12</sup> it leads to critical concentrations close to the experimental observations, we analyze here in more detail both the statistical mechanics of this model and its physical implications to the order-disorder transition in  $(\text{GaAs})_{1-x}\text{Ge}_{2x}$ .

We start by considering the consequences of a quenched disorder of species  $C$  in the pair probabilities

$p_{IJ}$  of the  $(AB)_{1-x}C_{2x}$  alloy. Since the distribution of species  $C$  is assumed to be uncorrelated with the occupation of neighboring sites, we introduce the following constraints to the BEG Hamiltonian of Eq. (1):

$$p_{CC} = x^2, \quad (6a)$$

$$p_{AC} + p_{BC} = 2x(1-x), \quad (6b)$$

$$p_{AA} + p_{BB} + p_{AB} = (1-x)^2. \quad (6c)$$

Here  $p_{SS'}$  for  $S \neq S'$  denotes the “nonoriented” pair probability for finding either  $S$ - $S'$  or  $S'$ - $S$  pairs.

A phase diagram for this model in the cluster-variation method can be more efficiently obtained by working with correlation functions as the independent variables for the free-energy minimization (instead of using the more straightforward “natural iteration” procedure<sup>12</sup>). The three constraints of Eqs. (6a)–(6c) and an additional constraint for a fixed concentration of species  $A$  or  $B$  [given by  $(1-x)/2$ ] reduce the number of independent  $\{p_{SS'}\}$  to two. Indeed, all pair probabilities can be expressed in terms of the concentration  $x$  and of the short-range-order (SRO) parameters

$$\sigma_1 = \frac{\langle S_i S_j \rangle}{(1-x)^2}, \quad \sigma_2 = \frac{\langle S_i S_j^2 + S_i^2 S_j \rangle}{2x(1-x)}, \quad (7)$$

where  $\langle \dots \rangle$  represents a thermodynamic average of nearest-neighbor spin products. The Hamiltonian of Eq. (1) then leads to the total energy per site at a given state of SRO  $\{\sigma\}$  in the form

$$E/N = 2(1-x)^2 \sigma_1 J + 2(1-x)^2 K + 4x(1-x) \sigma_2 L. \quad (8)$$

Notice that the  $K$  term is constant at a given concentration and therefore does not influence either the ground state or the thermodynamic properties of such a model. Since the BEG Hamiltonian is invariant under the interchange  $L \leftrightarrow -L$  and  $S_i \leftrightarrow -S_i$ , for all sites  $i$ , the phase diagram must be symmetric about  $L = 0$ .

We analyze now the ground-state properties of this model. The first step is to minimize Eq. (8) with respect to the SRO parameters  $\{\sigma\}$  with the constraints of Eqs. (6a)–(6c). This is a simple linear programming problem.<sup>22</sup> For  $J > 0$  and  $L \geq 0$ , there are two classes of solutions: (i) if  $L/J < 1$ ,

$$\sigma_1 = -1, \quad \sigma_2 = 0; \quad (9)$$

(ii) if  $L/J > 1$ ,

$$\sigma_1 = \begin{cases} (3x-1)/(1-x) & \text{for } x \leq \frac{1}{2} \\ 1 & \text{for } x \geq \frac{1}{2}, \end{cases} \quad (10)$$

$$\sigma_2 = \begin{cases} -1 & \text{for } x \leq \frac{1}{2} \\ -(1-x)/x & \text{for } x \geq \frac{1}{2}. \end{cases}$$

A transition between these two classes of ground states occurs at  $L/J = 1$ , which corresponds precisely to the

value obtained with the UPTB parameters (Table II). For exactly  $L/J = 1$ , the energy degeneracy between the two types of ground states is removed by maximizing the CVM pair-approximation entropy.<sup>23</sup> The nonoriented pair probabilities  $p_{SS'}$  can be expressed in terms of  $x$  and  $\{\sigma\}$  and are displayed in Fig. 3 for the case  $L > 0$ . (The curves for  $L < 0$  are the same as for  $L > 0$  if one changes  $\text{Ga} \leftrightarrow \text{As}$ .) By contrast, if we assume total equilibration of the original BEG model and the UPTB parameters of Table II, only Ga-As and Ge-Ge bonds are significantly present at  $T \lesssim 1000$  K.

It is worth remarking that these results indicate the total absence of Ga-Ga bonds but a significant number of As-As bonds (solid lines in Fig. 3) for  $L/J \geq 1$ . At typical preparation temperatures and with the UPTB values of  $J$  and  $L$ , the CVM pair probabilities are almost identical to the  $T=0$  results displayed in Fig. 3 for  $L/J=1$ . The fraction of As-As bonds reaches 8.7% at  $x = \frac{1}{4}$ . The presence of such wrong bonds in  $(\text{GaAs})_{1-x}\text{Ge}_{2x}$  has been the subject of controversy. Electronic-structure calculations<sup>24,25</sup> show that a significant number of As-As bonds should close the energy gap of the alloy over a wide composition range, contrary to experiment.

This ground-state analysis has determined the (*exact* for  $L/J < 1$  and  $L/J > 1$ )  $T = 0$  values of the SRO parameters  $\{\sigma\}$  as a function of the BEG interactions and concentration  $x$  of species  $C$ . This is a result of the fact that the total energy depends only on SRO. To describe the state of *long-range* order (LRO), however, we need to introduce new parameters that indicate the possible different occupation of the two fcc sublattices  $\alpha$  and  $\beta$

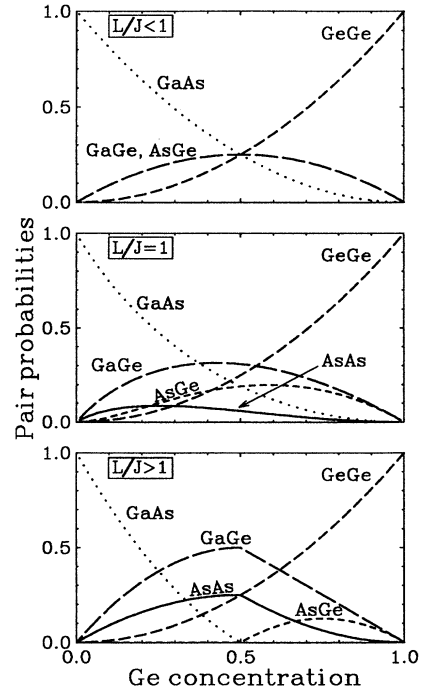


FIG. 3. Nonoriented nearest-neighbor pair probabilities in the ground state of the quenched-disorder model for  $(\text{GaAs})_{1-x}\text{Ge}_{2x}$  with  $L \geq 0$ .

by the three species. Two LRO parameters, involving the site and nearest-neighbor pair, are necessary. They can be chosen to be

$$\eta_1 = \frac{\langle S_i \rangle - \langle S_j \rangle}{2(1-x)}, \quad \eta_2 = \frac{\langle S_i S_j^2 - S_i^2 S_j \rangle}{2(1-x)}, \quad (11)$$

where  $i$  and  $j$  are sites on the  $\alpha$  and  $\beta$  sublattices, respectively, and are nearest neighbors in the definition of  $\eta_2$ . The LRO parameters  $\{\eta\}$  are zero in the diamond phase and nonzero in the zinc-blende phase. The oriented pair probabilities  $y_{SS'}^{\alpha\beta}$ , i.e, the probability of finding species  $S$  on the  $\alpha$  sublattice site and species  $S'$  on the  $\beta$  sublattice site of a nearest-neighbor pair of sites, can then be expressed in terms of the concentration  $x$ , the SRO parameters  $\{\sigma\}$ , and the LRO parameters  $\{\eta\}$ . In the CVM pair approximation, the configurational entropy  $S$  is a function of  $\{y_{SS'}^{\alpha\beta}\}$  only. It can therefore be expressed as a function of  $x$ ,  $\{\sigma\}$ , and  $\{\eta\}$ . At given values of the interaction parameters, the concentration  $x$ , and the temperature  $T$ , the thermodynamics is determined by minimizing the free energy

$$F(\{\sigma\}, \{\eta\}) = E(\{\sigma\}) - TS(\{\sigma\}, \{\eta\}) \quad (12)$$

with respect to  $\{\sigma\}$  and  $\{\eta\}$ . Notice that the limiting behavior of the system as  $T \rightarrow 0$  is obtained by first minimizing  $E(\{\sigma\})$  [leading to the solution given in Eqs. (9) and (10)] and then, for these  $\{\sigma\}$ , by maximizing  $S(\{\sigma\}, \{\eta\})$  with respect to  $\{\eta\}$  only. It is clear that this procedure must lead to a constant value of the critical concentration  $x_c$  in each of the two intervals  $0 < L/J < 1$  and  $L/J > 1$ , corresponding to the two ground-state solution of Eqs. (9) and (10), and possibly a different  $x_c$  at exactly  $L/J = 1$ . In the CVM pair approximation the result turns out to be

$$x_c = \begin{cases} \frac{2}{3} & \text{for } |L|/J < 1 \\ \frac{3}{8} & \text{for } |L|/J = 1 \\ \frac{1}{6} & \text{for } |L|/J > 1. \end{cases} \quad (13)$$

When  $L = 0$ , the quenched-disorder model corresponds to the dilute (spin- $\frac{1}{2}$ ) Ising model,<sup>26</sup> which is a simple representation of a system of interacting magnetic ions distributed at random in a given lattice with concentration  $p = 1 - x$ . The  $T \rightarrow 0$  limit of this system corresponds to the purely geometrical site-percolation problem. For the diamond lattice, the best numerical result for the percolation threshold is  $p_c^{\text{exact}} = 0.43$  (Ref. 27); thus, at  $L = 0$ ,  $x_c^{\text{exact}} = 1 - p_c^{\text{exact}} = 0.57$ , compared to the CVM result  $x_c^{\text{CVM}} = \frac{2}{3}$ . The discussion of the preceding paragraph shows that this value should persist for all  $|L|/J < 1$ . Although the CVM error in the critical concentration at  $T = 0$  (17%) is somewhat larger than the error in the critical temperature at  $x = 0$  (6.7%), the general shape of the order-disorder transition curve of the dilute Ising model<sup>26</sup> is reproduced by CVM, as shown in the next section. The CVM results, together with the knowledge of the exact  $T = 0$  results, give therefore reliable information about the quenched-disorder model at low temperatures.

## V. PHASE DIAGRAM OF THE QUENCHED-DISORDER MODEL

At a given  $L/J$  and  $k_B T/J$ , the critical concentration  $x_c$  is the value of  $x$  where the free energy ceases to be a minimum and becomes a maximum in the disordered (diamond) phase, where  $\eta_1 = \eta_2 = 0$ . This implies that, at  $x = x_c$ , the determinant of the Hessian (the matrix of the second derivatives of  $F$  with respect to the four order parameters) is zero. In the disordered phase this matrix is block diagonal (the elements related to LRO-SRO cross terms are zero) so we need only to solve for the root  $x = x_c$  of the determinant of the  $2 \times 2$  part of the Hessian related to the LRO parameters:

$$\det \left( \frac{\partial^2 F}{\partial \eta_i \partial \eta_j} \right)_{\eta_1 = \eta_2 = 0} = 0, \quad (14)$$

where the values of  $\sigma_1$  and  $\sigma_2$  in  $F$  are obtained by taking  $\partial F / \partial \sigma_i = 0$ .

The phase diagram of Fig. 4 is efficiently obtained by repeating this procedure for different values of  $L/J$  and  $k_B T/J$ . Notice the rapid variation of  $x_c$  with respect to  $L/J$  for  $|L|/J \sim 1$  and  $k_B T/J \lesssim 0.5$ . This is necessary for a smooth joining of the finite-temperature transition surface with the ground-state discontinuous transition line, given by Eq. (13). Another remarkable characteristic of our phase diagram is the strong reentrant behavior of the transition curve for  $L/J$  slightly less than 1. In this regime, for  $x$  slightly larger than  $x_c = \frac{1}{6}$ , a disorder  $\rightarrow$  order transition precedes the order  $\rightarrow$  disorder transition as  $T$  increases.

We highlight the transition line corresponding to the  $(\text{GaAs})_{1-x}\text{Ge}_{2x}$  UPTB parameters ( $L/J = 1.00$ ), which reproduces the phase diagram shown by Gu, Ni, and Zhu.<sup>12</sup> The constant- $L$  curves displayed near  $L/J = 1.00$  correspond to  $L/J = 0.95$  and  $1.05$ . To illustrate the sensitivity of the critical concentration with  $L/J$ , we also highlight the isotherm (horizontal cross section) of the phase diagram at  $k_B T/J = 0.4$ , which, at the preparation temperature  $T = 700$  K, corresponds to the parameter  $J = 149$  meV found by Gu, Ni, and Zhu. This isotherm and that for  $k_B T/J = 0.32$ , which corresponds

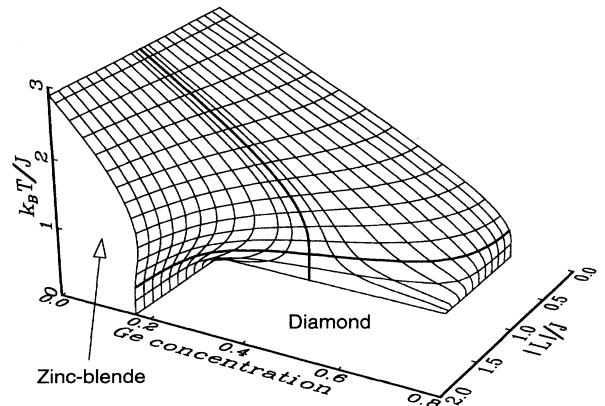


FIG. 4. Phase diagram of the quenched-disorder model.

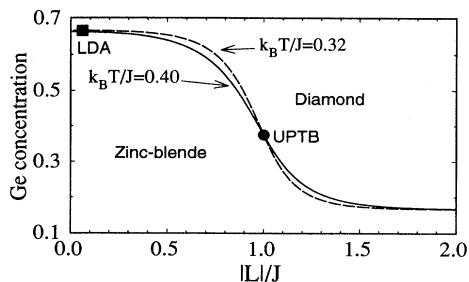


FIG. 5. Two isotherms of the phase diagram of Fig. 4, corresponding to the preparation temperature 700 K and values of  $J$  obtained by Gu, Ni, and Zhu (Ref. 12) (solid line) and in the present work (dashed line). The circle (UPTB) and the square (LDA) indicate the values of  $|L|/J$  obtained in Ref. 12 and in the present work, respectively.

to our parameter  $J = 189$  meV, are displayed in Fig. 5 together with the points corresponding to values of  $L/J = 1.00$  (UPTB, Ref. 12) and  $-0.06$  (LDA, this work). For  $k_B T/J = 0.4$ ,  $x_c$  decreases from 0.54 to 0.24 as  $L$  changes only from 0.8 to 1.2, which is a fluctuation certainly within the error incurred by the UPTB parameters.

Our results (marked LDA in Fig. 5) indicate that the critical concentration shows a negligible variation with respect to the  $T=0$ ,  $L=0$  value  $x_c = 0.67$ . The  $L=0$  limit makes the quenched-disorder model equivalent to the dilute spin- $\frac{1}{2}$  Ising antiferromagnet with a concentration  $p = 1 - x$  of the magnetic species. The CVM pair approximation reproduces correctly the qualitative features of the phase diagram for this dilute Ising antiferromagnet, which corresponds to the  $L=0$  cross section of the three-dimensional phase diagram of Fig. 4, including the “percolation threshold”  $p_c = 1 - x_c$  (below which only a disordered phase exists at  $T=0$ ) and the vertical slope of the transition curve as  $T \rightarrow 0$ . This last feature and the very small changes apparent in our transition curves (Fig. 4) when  $|L|/J$  is changed from 0 to 0.06 lead us to conclude that our interaction parameters correspond to a true critical concentration  $x_c \approx 1 - p_c^{\text{exact}} = 0.57$ , at  $T \approx 700$  K, in disagreement with the value  $x_c = 0.36$  obtained by Gu, Ni, and Zhu<sup>12</sup> and with the experimental result  $x_c = 3-4$ .<sup>4,5</sup> This suggests that the quenched-disorder model is inadequate to describe the correct nature of the distribution of Ga, As, and Ge atoms in  $(\text{GaAs})_{1-x}\text{Ge}_{2x}$  alloys.

## VI. CONCLUSIONS

We obtained in this work the “wrong-bond” interaction energy and the Ga $\leftrightarrow$ As asymmetry parameter  $L$ , complementing our previous determination of interaction parameters in a spin-1 Ising (Blume-Emery-Griffiths) representation of  $(\text{GaAs})_{1-x}\text{Ge}_{2x}$  alloys. This was accomplished by fitting the spin-1 Hamiltonian to the total energies of ordered structures calculated by the

first-principles pseudopotential method, using the local-density approximation (LDA). We find  $L = -11$  meV, which implies a slight preference for Ga-Ga bonds over As-As bonds, in disagreement with the results obtained with universal-parameter tight-binding (UPTB) interactions.

We then reexamined the thermodynamic consequences of a recently proposed quenched-disorder model for  $(\text{GaAs})_{1-x}\text{Ge}_{2x}$  in which Ge atoms are distributed at random in the alloy. This corresponds to a generalization of the dilute Ising antiferromagnetic model. A complete three-dimensional phase diagram in the  $(x, L/J, k_B T/J)$  space was determined in the pair approximation of the cluster-variation method (CVM). Interesting features included a discontinuity at  $T = 0$  and a strong reentrant behavior. We showed that the UPTB parameters correspond to a special region of the phase diagram where the critical curve is very sensitive to the values of the interaction parameters. We estimated that our interaction parameters correspond to a critical concentration  $x_c = 0.57$  in the quenched-disorder model.

We summarize in Table III the main results of the application of thermodynamic models to  $(\text{GaAs})_{1-x}\text{Ge}_{2x}$  alloys. The first column shows that, without “wrong” ( $\Delta Z_v = \pm 2$ ) bonds, the critical concentration has a lower boundary 0.57 in the CVM pair approximation. This limit corresponds to a correlated three-species percolation problem, where Ge, Ga, and As atoms are distributed at random in a diamond lattice with the provision that no Ga-Ga or As-As nearest-neighbor pairs occur. This is different from the simpler “classical” two-species percolation problem,<sup>28</sup> with Ge and “non-Ge” atoms distributed at random. In this classical percolation problem, formation of Ga-As ordered clusters can be assumed to occur *after* Ge atoms are distributed at random. This corresponds to the  $T \rightarrow 0$  limit of the  $L=0$  quenched-disorder model, discussed in Sec. IV (with  $x_c = \frac{2}{3}$  in the CVM pair approximation). The agreement between the CVM value for the three-species percolation problem and the *exact* value  $x_c^{\text{exact}} = 1 - p_c^{\text{exact}} = 0.57$  for the classical percolation problem seems to be fortuitous. In analogy with the classical percolation problem, it is expected that  $x_c$  for the three-species problem without wrong bonds will be lowered somewhat if the statistical approximation is improved. With LDA interaction parameters, however, the assumption of no wrong bonds leads to phase separation at all temperatures below melting.

Column two of Table III shows that, while adjustable interaction parameters can lead to  $x_c \approx 0.3$  if wrong bonds are allowed (i.e.,  $E_w < \infty$ ), we found<sup>6</sup> that using first-principles LDA interactions leads again to phase separation. This occurs because the average lowest-energy nonoctet bonds (the “bad” bonds, with  $\Delta Z_v = \pm 1$ ) are still  $\gtrsim 100$  meV higher in energy than the normal Ga-As and Ge-Ge bonds. Column three of Table III shows that using realistic LDA values for  $E_w < \infty$  and  $L \neq 0$  does not affect this result. A similar result is found when UPTB parameters are used in a total-equilibration model. On the other hand, column four shows that a quenched-disorder model coupled to UPTB parameters leads to



TABLE III. Summary of results obtained with thermodynamic models for  $(\text{GaAs})_{1-x}\text{Ge}_{2x}$  alloys. The parameters  $E_w$  and  $L$  are the “wrong-bond” ( $\Delta Z_v = \pm 2$ ) average energy and the Ga $\leftrightarrow$ As asymmetry parameter, respectively. The symbol  $x_c$  represents the critical concentration for the zinc-blende to diamond phase transition and PS indicates phase separation.

Parameters	$L=0, E_w \rightarrow \infty$	$L=0, E_w < \infty$	$L \neq 0, E_w < \infty$	QD <sup>a</sup>
Adjustable <sup>b</sup>	$x_c \geq 0.57$	$x_c \approx 0.3$		
UPTB <sup>c</sup>			PS	$x_c = 0.36$
LDA <sup>d</sup>	PS	PS	PS	$x_c = 0.57$

<sup>a</sup> Quenched disorder.

<sup>b</sup> References 10 and 11 in the CVM pair approximation. The value  $x_c \approx 0.3$  corresponds to  $k_B T/J \approx 2$ .

<sup>c</sup> Universal parameter tight binding, Ref. 12, with  $T \approx 700$  K in the CVM pair approximation.

<sup>d</sup> First-principles local-density approximation, Ref. 6 and the present work. No significant changes from the phase diagram of Ref. 6 ( $L=0, E_w \rightarrow \infty$ ) occur at  $T \lesssim 1500$  K using LDA parameters  $E_w < \infty$  or  $L \neq 0$ . The critical concentration  $x_c$  for QD is a good estimate of the exact value at  $T \approx 700$  K, as discussed in the text.

$x_c = 0.36$  in the CVM pair approximation. We showed in this paper, however, that this result is a consequence of the empirical UPTB parameters used. First-principles parameters lead to  $x_c = 0.67$  in the CVM pair approximation, and an estimated near-exact value  $x_c = 0.57$ . This is in disagreement with the experimental values  $x_c = 0.3-0.4$ .

We conclude that the quenched-disorder model, like the other thermodynamic models, does not describe correctly the arrangement of atoms in  $(\text{GaAs})_{1-x}\text{Ge}_{2x}$ . Further evidence for this conclusion can be found in the anisotropic nature of the experimental samples as determined by transmission electron microscopy (TEM).<sup>29</sup> Ordered domains are observed to extend along the direction parallel to growth. This feature is absent in the quenched-disorder model, which is isotropic. Anisotropy is captured by growth models,<sup>24,30,31</sup> which are based on “growth rules,” not obviously related to thermody-

namics, but designed to reproduce the observed critical concentration. It is possible, however, that partial thermal equilibration of the *reconstructed* free surface (rather than the bulk) during growth plays a role in determining the final structure of the alloy. Such a mechanism was recently proposed<sup>32</sup> to explain spontaneous “CuPt” ordering in  $\text{Ga}_{1-x}\text{In}_x\text{P}$ .

#### ACKNOWLEDGMENTS

We thank Alex Zunger for very useful discussions and suggestions. This work was supported in part by the U.S. Department of Energy, Office of Energy Research, Basic Energy Science Grant No. DE-AC02-83CH10093. One of us (R.O.) would like to thank Conselho Nacional de Desenvolvimento Científico e Tecnológico (Brazil) for support.

\*Permanent address: Departamento de Física, Universidade de Brasília, 70910 Brasília, Distrito Federal, Brazil.

<sup>1</sup>Y. Takada, T. Hirai, and M. Hirao, *J. Electrochem. Soc.* **112**, 363 (1965).

<sup>2</sup>J. E. Greene, *J. Vac. Sci. Technol. B* **1**, 229 (1983).

<sup>3</sup>K. E. Newman and J. D. Dow, *Phys. Rev. B* **27**, 7495 (1983).

<sup>4</sup>I. Banerjee, D. W. Chung, and H. Kroemer, *Appl. Phys. Lett.* **46**, 494 (1985).

<sup>5</sup>S. I. Shah, B. Kramer, S. A. Barnett, and J. E. Greene, *J. Appl. Phys.* **59**, 1482 (1986).

<sup>6</sup>(a) R. Osório, S. Froyen, and A. Zunger, *Solid State Commun.* **78**, 249 (1991); (b) *Phys. Rev. B* **43**, 14055 (1991).

<sup>7</sup>M. A. Davidovich, B. Koiller, R. Osório, and M. O. Robbins, *Phys. Rev. B* **38**, 10524 (1988).

<sup>8</sup>T. Ito, *Jpn. J. Appl. Phys.* **27**, 1916 (1988).

<sup>9</sup>S. Lee, D. M. Bylander, and L. Kleinman, *Phys. Rev. B* **41**, 10264 (1990).

<sup>10</sup>B. Koiller, M. A. Davidovich, and R. Osório, *Solid State Commun.* **55**, 861 (1985).

<sup>11</sup>B.-L. Gu, K. E. Newman, and P. A. Fedders, *Phys. Rev. B* **35**, 9135 (1987).

<sup>12</sup>B.-L. Gu, J. Ni, and J.-L. Zhu, *Phys. Rev. B* **45**, 4071 (1992).

<sup>13</sup>W. A. Harrison and E. A. Kraut, *Phys. Rev. B* **37**, 8244 (1988).

<sup>14</sup>D. Mukamel and M. Blume, *Phys. Rev. A* **10**, 610 (1974). The complete corrected equations for this mapping are found in Appendix B of Ref. 6(b).

<sup>15</sup>M. Blume, V. J. Emery, and R. B. Griffiths, *Phys. Rev. A* **4**, 1071 (1971).

<sup>16</sup>M. Tanaka and T. Kawabe, *J. Phys. Soc. Jpn.* **54**, 2194 (1985).

<sup>17</sup>R. Osório, M. J. de Oliveira, and S. R. Salinas, *J. Phys. Condens. Matter* **1**, 6887 (1989).

<sup>18</sup>D. B. Laks, R. Magri, and A. Zunger, *Solid State Commun.* **83**, 21 (1992).

<sup>19</sup>D. Vanderbilt and C. Lee, *Phys. Rev. B* **45**, 11192 (1992).

<sup>20</sup>R. G. Dandrea, S. Froyen, and A. Zunger, *Phys. Rev. B* **42**, 3213 (1990).



- <sup>21</sup>Q.-M. Zhang, G. Chiarotti, A. Selloni, R. Car, and M. Parrinello, *Phys. Rev. B* **42**, 5071 (1990).
- <sup>22</sup>See, for instance, F. Ducastelle, *Order and Phase Stability in Alloys* (North-Holland, Amsterdam, 1991), Chap. 3.
- <sup>23</sup>R. Kikuchi, *Phys. Rev.* **81**, 988 (1951).
- <sup>24</sup>L. C. Davis and H. Holloway, *Phys. Rev. B* **35**, 2767 (1987).
- <sup>25</sup>K. C. Hass and R. J. Baird, *Phys. Rev. B* **38**, 3591 (1988).
- <sup>26</sup>See, for instance, R. B. Stinchcombe, in *Phase Transitions and Critical Phenomena*, edited by C. Domb and J. B. Lebowitz (Academic, London, 1983), Vol. 7, Chap. 3.
- <sup>27</sup>A. Silverman and J. Adler, *Phys. Rev. B* **42**, 1369 (1990).
- <sup>28</sup>See, for instance, D. Stauffer, *Introduction to Percolation Theory* (Taylor & Francis, London, 1985), Sec. 2.4.
- <sup>29</sup>T. C. McGlinn, M. V. Klein, L. T. Romano, and J. E. Greene, *Phys. Rev. B* **38**, 3362 (1988).
- <sup>30</sup>K. Kim and E. A. Stern, *Phys. Rev. B* **32**, 1019 (1985).
- <sup>31</sup>R. B. Capaz, G. F. Preger, and B. Koiller, *Phys. Rev. B* **40**, 8299 (1989).
- <sup>32</sup>S. Froyen and A. Zunger, *Phys. Rev. Lett.* **66**, 2132 (1991); R. Osório, J. E. Bernard, S. Froyen, and A. Zunger, *Phys. Rev. B* **45**, 11 173 (1992).